

1  
2  
3  
4  
5  
6  
7  
8  
9  
10  
11  
12  
13  
14       **A red tide of *Alexandrium fundyense* in the Gulf of Maine**  
15

16                     D.J. McGillicuddy, Jr.<sup>a</sup>  
17                     M.L. Brosnahan<sup>b</sup>  
18                     D.A. Couture<sup>c</sup>  
19                     R. He<sup>d</sup>  
20                     B.A. Keafer<sup>b</sup>  
21                     J.P. Manning<sup>e</sup>  
22                     J.L. Martin<sup>f</sup>  
23                     C.H. Pilskaln<sup>g</sup>  
24                     D.W. Townsend<sup>h</sup>  
25                     D.M. Anderson<sup>b</sup>  
26  
27

28       Manuscript revised and resubmitted to *Deep-Sea Research II*  
29

30                     April 15, 2013  
31  
32

33       <sup>a</sup>Department of Applied Ocean Physics and Engineering, Woods Hole Oceanographic Institution,  
34 Woods Hole, MA 02543, USA. Tel: 508-289-2683 Fax: 508-457-2194 Email:  
35 dmgillicuddy@whoi.edu (Corresponding Author).

36       <sup>b</sup>Biology Department, Woods Hole Oceanographic Institution, Woods Hole, MA 02543, USA.

37       <sup>c</sup>Resource Access International, Brunswick, ME 04011, USA.

38       <sup>d</sup>Department of Marine, Earth, and Atmospheric Sciences, North Carolina State University,  
39 Raleigh, NC 27695, USA.

40       <sup>e</sup>National Oceanic Atmospheric Administration, Northeast Fisheries Science Center, Woods  
41 Hole, MA 02543, USA

42       <sup>f</sup>St. Andrews Biological Station, Fisheries and Oceans Canada, St. Andrews, NB E5B 2L9,  
43 Canada.

44       <sup>g</sup>School of Marine Sciences, University of Massachusetts Dartmouth, North Dartmouth, MA  
45 02747, USA.

46       <sup>h</sup>School of Marine Sciences, University of Maine, Orono, ME 04469, USA.

47  
48  
49  
50  
51

## Abstract

In early July 2009, an unusually high concentration of the toxic dinoflagellate *Alexandrium fundyense* occurred in the western Gulf of Maine, causing surface waters to appear reddish brown to the human eye. The discolored water appeared to be the southern terminus of a large-scale event that caused shellfish toxicity along the entire coast of Maine to the Canadian border. Rapid-response shipboard sampling efforts together with satellite data suggest the water discoloration in the western Gulf of Maine was a highly ephemeral feature of less than two weeks in duration. Flow cytometric analysis of surface samples from the red water indicated the population was undergoing sexual reproduction. Cyst fluxes downstream of the discolored water were the highest ever measured in the Gulf of Maine, and a large deposit of new cysts was observed that fall. Although the mechanisms causing this event remain unknown, its timing coincided with an anomalous period of downwelling-favorable winds that could have played a role in aggregating upward-swimming cells. Regardless of the underlying causes, this event highlights the importance of short-term episodic phenomena on regional population dynamics of *A. fundyense*.

67

68  
69  
70

71 Key words: Phytoplankton; Population dynamics; Red tides; Cysts; Paralytic shellfish poisoning;  
72 USA, Gulf of Maine.

73     **1. Introduction**

74         Although the term “red tide” is frequently used in reference to harmful algal bloom  
75         events, its use to describe blooms of *Alexandrium fundyense* in the Gulf of Maine is largely a  
76         misnomer. Concentrations of *A. fundyense* seldom reach levels sufficient to discolor the water,  
77         and this species typically constitutes a small fraction of the total phytoplankton biomass.  
78         However, there have been some exceptions, including the historic bloom of 1972 during which  
79         *A. fundyense* (formerly *Gonyaulax tamarensis*) discolored the water offshore of the northern  
80         Massachusetts and New Hampshire coastlines (Hartwell, 1975; Mulligan, 1973; Sasner et al.,  
81         1974). *A. fundyense* also discolored water in the Bay of Fundy in 1980, 2003, and 2004 (Martin  
82         et al., 2008; Martin and White, 1988).

83         An unusual “red tide” of *A. fundyense* occurred in the Gulf of Maine in 2009. Initial  
84         discovery of the anomaly was serendipitous, taking place on a mooring turnaround cruise  
85         prompted by an increase in Paralytic Shellfish Poisoning (PSP) toxicity along the Maine coast in  
86         late June - early July. Visual observations of discolored water prompted surface sampling to  
87         and from the mooring site, revealing *A. fundyense* concentrations ranging from hundreds of  
88         thousands of cells l<sup>-1</sup> to in excess of one million cells l<sup>-1</sup>. This triggered a rapid-response  
89         sampling effort, both at sea and via aerial survey. Herein we characterize the phenomenology of  
90         this event utilizing these observations together with satellite imagery, shellfish toxicity  
91         measurements, flow cytometric analysis of samples from the discolored water, as well as cyst  
92         fluxes from a nearby sediment trap and a spatial survey of cysts in coastal sediments the  
93         following October. Through synthesis of this diverse set of observations, it is clear this was a  
94         significant event not only in terms of coastal shellfish toxicity, but also the regional population  
95         dynamics of *A. fundyense*.

96     **2. Methods**

97

98     *2.1 Hydrography*

99                 Hydrographic profiles and water samples were collected with a standard CTD-rosette  
100        system with Niskin bottles. *A. fundyense* samples were collected by sieving 2 l through a 20 µm  
101        Nitex screen that was washed into a 15 ml centrifuge tube and fixed in 5% formalin for <24  
102        hours. The samples were then centrifuged, the supernatant removed, and ice-cold methanol  
103        added. Samples were stored at -20°C for later enumeration in the laboratory (section 2.2 below).  
104        An additional 10 l sample of surface water was sieved in the same manner for the purposes of an  
105        on-board “live” count. Nutrient samples were filtered through Millipore HA filters, placed  
106        immediately in a sea water-ice bath for 5–10 min, and frozen at -18°C. Concentrations of  
107        NO<sub>3</sub>+NO<sub>2</sub>, NH<sub>4</sub>, Si(OH)<sub>4</sub> and PO<sub>4</sub> were measured ashore following each cruise with a Bran  
108        Luebbe AA3 AutoAnalyzer using standard techniques.

109

110     *2.2 Moored observations*

111                 A McLane Laboratories Inc. autonomous Phytoplankton Sampler (PPS) obtained  
112        measurements at 5 m depth from April to September in two contiguous deployments. The  
113        mooring was located in the vicinity of the Northeastern Regional Association of Coastal and  
114        Ocean Observing Systems (NERACOOS) buoy B at 43° 11'N, 70° 26'W (Figure 1, “B”). A  
115        total of 24 samples were taken per deployment, at a frequency of one every 2-3 days. For each  
116        sample, the instrument filters 2 l of seawater onto a 15 µm Nitex screen. The instrument was  
117        prepared with 10% formalin dissolved in artificial seawater that was adjusted to be lighter  
118        (specific density= 1.018) than the ambient sample seawater. During the automated filtering

119 process, the “light” 10% formalin solution dispensed into the bottom of the filter reservoirs is  
120 diluted and displaced upward onto the filter by the heavier ambient sample seawater. This  
121 process resulted in a  $\frac{1}{2}$  reduction in the concentration of preservative to about 5% final. After  
122 the instrument was recovered, the preserved  $>15 \mu\text{m}$  samples were backwashed off the Nitex  
123 screen into a 50 ml centrifuge tube for further concentration and *A. fundyense* cell counting as  
124 described in the following section.

125

126 *2.3 Enumeration of A. fundyense cells and cysts*

127 *A. fundyense* cells were enumerated from water samples using a species-specific  
128 oligonucleotide probe and methods described in Anderson et al. (2005c). Both *A. tamarensis* and  
129 *A. fundyense* occur in the Gulf of Maine, and these are considered to be varieties of the same  
130 species (Anderson et al., 1994; Brosnahan et al., 2010; Scholin et al., 1995). Available molecular  
131 probes cannot distinguish between them, and only detailed analysis of the thecal plates on  
132 individual cells can provide this resolution—which is not practical for large numbers of field  
133 samples. Accordingly, for the purpose of this study, the name *A. fundyense* is used to refer to  
134 both forms.

135 Surface “live” counts consisted of two transects across a Sedgewick-Rafter counting slide  
136 using an on-board light microscope at 200 x magnification. The slide was loaded with 1 ml of  
137 concentrated sieved material (see section 2.1 above) resuspended to 14 ml. This provided a lower  
138 limit of detection of 14 cells  $\text{l}^{-1}$ . Light microscopy of this kind cannot distinguish *A. fundyense*  
139 from the morphologically similar non-toxic species *A. ostenfeldii*, and therefore the live counts  
140 can sometimes overestimate *A. fundyense* concentration.

141 Cysts of *A. fundyense* were collected and enumerated from sediment samples using  
142 primulin-staining methods described in Anderson et al. (2005d). Samples were obtained with a  
143 Craib corer in dedicated surveys in fall 2008, 2009, and 2010. The sampling pattern consisted of  
144 14 cross-shore transects in the coastal Gulf of Maine and three transects across Georges Bank,  
145 for a total of approximately 120 stations. *A. fundyense* cysts from the upper 1 cm of oxygenated  
146 sediment are viable for germination (Anderson et al., 2005d) and thus only that vertical fraction  
147 of the sediment samples is presented herein.

148 Cyst fluxes were measured in time-series sediment traps (Honjo and Doherty, 1988)  
149 deployed on subsurface moorings. See Pilskaln et al. (this issue) for a complete description of  
150 these data. Of particular interest to this study are the traps located in Wilkinson Basin located at  
151 42° 43'N, 69° 58'W (Figure 1, "WB"). The traps had a baffled surface collection area of 0.5  
152 m<sup>2</sup>, and collected time-series samples in thirteen 250 ml volume cups per deployment. Prior to  
153 deployment, trap cups were pre-poisoned with an 8% density-adjusted formalin solution in  
154 filtered seawater buffered to a pH of 8.0-8.1. Recovery and redeployment of the trap moorings  
155 occurred approximately every 5-9 months, with individual cup collection periods varying from  
156 ~10-20 days. The traps were programmed to insure that the cups on the upper and lower traps  
157 rotated and collected sinking particulate material on the same time interval. Trap samples were  
158 processed by removing the formalin solution with sieving through a 20 µm Nitex screen. The  
159 material retained on the screen was then treated as a sediment sample using the same primulin-  
160 staining protocols noted above (Anderson et al., 2005d). Only primulin-labeled, capsule-shaped  
161 cysts with intact internal cellular contents were counted; empty cysts were not quantified.

162  
163

164        2.4 Flow Cytometric Analysis

165              Subsamples of 10,000 cells from surface samples taken on the July 10 mooring

166              turnaround cruise and from a log-phase laboratory culture of a Gulf of Maine *A. fundyense*

167              isolate (clone 38-3) were stained with propidium iodide (PI) for DNA content analysis by flow

168              cytometry. All of the samples were fixed with 5% formalin and resuspended in ice-cold

169              methanol prior to staining. Methanol was removed by centrifuging the cell suspensions for 10

170              minutes at 3,000 rcg then aspirating the methanol supernatant. The cell pellets were then washed

171              by resuspension in 1 ml of PBS (40 mM Na<sub>2</sub>HPO<sub>4</sub>, 22 mM KH<sub>2</sub>PO<sub>4</sub>, 85 mM NaCl), and

172              centrifuged again for 10 minutes at 3,000 rcg. The overlying PBS solution was then aspirated

173              before the cells were stained in PBS amended with 4 µg ml<sup>-1</sup> PI and 100 Kunitz ml<sup>-1</sup> RNase A

174              for at least 3 hours in darkness and at room temperature. At least 2,000 particles having PI-

175              associated fluorescence comparable to *A. fundyense* culture cells were recorded from each field

176              sample with a FACSCalibur flow cytometer (BD Biosciences). These observations were used to

177              compute relative frequency distributions of FL2-H band (PI-associated) fluorescence, which

178              provides a quantitative measure of DNA content. All measurements were made with linear

179              signal amplification.

180              The DNA content of *A. fundyense* cells changes in a quantized fashion as they progress

181              through the phases of the cell division cycle (mitosis) and also the gamete and zygote stages of

182              its sexual life cycle. Haploid vegetative *A. fundyense* oscillate between 1c and 2c DNA content

183              as they undergo mitosis; 1c G1 phase cells become 2c G2 phase cells when they replicate their

184              DNA, then return to the 1c G1 phase when they divide. The G1 phase is long relative to the G2

185              phase in *A. fundyense* and divisions are often phased by the diel light/dark cycle, such that most

186              occur at daybreak (Rubin, 1981; Taroncher-Oldenburg et al., 1997). As a consequence, growing

187 populations of *A. fundyense* tend to be dominated by 1c G1 phase cells, especially in the late-  
188 morning and afternoon (Brosnahan et al., this issue).

189 In contrast, sexual-phase cells do not oscillate between DNA content levels, but instead  
190 increase in DNA content as they progress from one stage to the next - first as 1c gametes, then as  
191 2c planozygotes – until eventually transforming to resting cysts and undergoing pre-meiotic  
192 replication to become 4c (or greater) in DNA content. The last transition to 4c DNA content has  
193 not been observed directly but is inferred from the resumption of mitosis by haploid, vegetative  
194 cells after cyst germination (Pfiester and Anderson, 1987). Because gametes have the same DNA  
195 content (1c) as G1 phase vegetative cells and planozygotes have the same content as G2 phase  
196 cells, DNA content alone cannot be used to determine the life cycle stage of an *A. fundyense* cell  
197 (Cetta and Anderson, 1990). However, the presence of a large fraction of 2c cells within a  
198 population can signal a shift from vegetative cell division to the formation of planozygotes,  
199 especially when high concentrations of 2c cells are observed during afternoon hours (Brosnahan  
200 et al., this issue).

201

## 202 2.5 Satellite observations

203 A variety of satellite data products were examined to determine their suitability for  
204 assessing the spatial and temporal scales of the red tide event. Of all that were considered, the  
205 Medium Resolution Imaging Spectrometer (MERIS) case 2 water algorithm for chlorophyll  
206 (Doerffer and Schiller, 2007) showed closest correspondence with the discolored water observed  
207 on July 10. Of course this algorithm is not specific to *A. fundyense*, and its relevance for this  
208 purpose is restricted only to those rare occasions when *A. fundyense* constitutes a significant  
209 fraction of the total phytoplankton biomass. There are many instances throughout the MERIS

210 data record when such imagery indicates the presence of high biomass during times when *A.*  
211 *fundyense* concentrations were known to be low (data not shown).

212

213 *2.6 Drifter tracks*

214 Surface drifters consisted of a 1.3m long, 0.8 cm diameter PVC cylinder (conventional  
215 pipe material) that supports two pairs of fiberglass rods. The rods were mounted radially and  
216 orthogonally to hold a set of four vinyl-cloth sails. The cylinder was ballasted so that only the  
217 GPS antenna and a small portion were exposed to the wind. While the design is essentially the  
218 same as the commercially available Davis-style (“CODE”) surface drifters (Davis, 1985), the  
219 electronics were replaced with new technology used for tracking vehicles on highways. The units  
220 were set to report every 0.5–2 h and communicate via the GLOBALSTAR satellite system.  
221 Drifter position data were processed to eliminate obvious bad points according to the methods  
222 described by Hansen and Poulain (1996). Data are available via the Open-source Project for a  
223 Network Data Access Protocol (OPeNDAP) at <http://www.nefsc.noaa.gov/epd/ocean>. For more  
224 information see Manning et al. (2009).

225

226 *2.7 Shellfish toxicity*

227 Shellfish toxicity measurements were based on the blue mussel *Mytilus edulis*, using the  
228 standard mouse bioassay (Association of Official Analytical Chemists, 1984; AOAC Official  
229 Method 959.08). These data were kindly provided by the Maine Department of Maine  
230 Resources (<http://www.state.me.us/dmr/>). A set of coastal locations are monitored on a weekly  
231 basis, and shellfish beds are closed when the mouse bioassay approaches the quarantine level of  
232 80 µg saxitoxin equivalents (STX) per 100 g of shellfish tissue.

233 **3. Results**

234

235 *3.1 Surface distributions of *A. fundyense* vegetative cells*

236         Surface samples collected in between Portsmouth NH and NERACOOS mooring B on 10  
237 July 2009 documented *A. fundyense* concentrations ranging from  $10^4$  cells l<sup>-1</sup> to in excess of  $10^5$   
238 cells l<sup>-1</sup> in offshore waters (Figure 1). *A. fundyense* was considerably less abundant in a near-  
239 shore sample, although the observed concentration of 25,690 cells l<sup>-1</sup> far exceeds the 200-1000  
240 cells l<sup>-1</sup> that typically leads to toxicity in shellfish sufficient to require regulatory closure in the  
241 region. These observations prompted a rapid-response survey cruise on board R/V *Tioga* on July  
242 12. Sampling consisted of (1) underway surface counts on a south-to-north line in transit to  
243 Cape Ann, (2) full hydrographic stations along a transect off Cape Ann, and (3) full  
244 hydrographic stations on the eastern half of a transect off Boston (Figure 1). Cell counts were  
245 low in Massachusetts and Cape Cod Bays. The western part of the Cape Ann line was devoid of  
246 cells, but offshore the numbers were high, peaking at over 7000 cells l<sup>-1</sup>. Due to time constraints  
247 it was not possible to delimit the offshore edge of the population, as the easternmost station was  
248 near 2000 cells l<sup>-1</sup>. Given the southward flow characteristic of this area, it seems logical to infer  
249 that this offshore population was connected with the extremely high concentrations in the  
250 discolored water observed along the coast to the north. In fact, the trajectory of a surface drifter  
251 released on July 9 just south of where the red water was observed on July 10 illustrates  
252 oceanographic connectivity between the two sets of observations on precisely the right time scale  
253 (Figure 1). Thus these data suggest the southern extent of the population had not been  
254 transported much further south than the Cape Ann line, at least in surface waters.

255           A regional-scale mapping effort was conducted on voyage #386 of R/V *Tioga* July 19-23.  
256   Cell counts were very low overall, with the 100 cells l<sup>-1</sup> threshold broken only in a few places  
257   along transects off Casco Bay, Isle au Haut, and Southwest Harbor (Figure 2). Fine-scale  
258   sampling of a near-coastal area with high toxicity (Southwest Harbor, Frenchman Bay, Winter  
259   Harbor, Schoodic Point, and Prospect Harbor) also failed to detect cell concentrations in excess  
260   of 200 cells l<sup>-1</sup> (Figure 2 inset). Nutrient concentrations were low throughout the region  
261   sampled during the survey, with dissolved nitrate plus nitrite concentrations at or below detection  
262   limits in the upper 10m (ca. 1.0 µM or less); however, ammonium concentrations were relatively  
263   high, reaching 2 µM at the surface and 10 m at the inner-most stations of the western gulf (not  
264   shown).

265

### 266   *3.2 Aerial survey*

267           Shipboard sampling on July 19 was accompanied by an aerial survey executed by spotter  
268   pilot Norman St. Pierre and observer Michael Brosnahan. Atmospheric conditions were ideal,  
269   and altitude was maintained at 200-500 m on tracks from the coast out to 10 km offshore. The  
270   survey spanned coastal areas from Cape Cod Bay to Bar Harbor, and water coloration indicative  
271   of high concentrations of *A. fundyense* was not found.

272

### 273   *3.3 Satellite observations*

274           A MERIS case 2 chlorophyll image from July 9 (Figure 3, top) indicates the presence of  
275   a chlorophyll anomaly precisely where the discolored water was observed on July 10. The  
276   region of enhanced chlorophyll extends along the coast southward to Cape Ann and northeast to  
277   the western side of Penobscot Bay. More modest enhancements are evident east of Penobscot

278 Bay along the Maine coast and up into the Bay of Fundy, although they appear as more isolated  
279 patches rather than a continuous feature. A time-series of images zoomed in on the region of  
280 discolored water illustrates the highly-ephemeral nature of this phenomenon (Figure 3, bottom).  
281 There was no trace of the feature on July 5, and isolated patches appeared on July 6.  
282 Concentrations peaked on July 9, and were on the decline by July 11. By July 12-15 the surface  
283 expression had completely disappeared.

284

285 *3.4 Toxicity measurements*

286 As of the week of June 15, PSP toxicity patterns observed along the Maine coast were  
287 fairly typical: toxicity was on the decline in western Maine, and had yet to rise in eastern Maine  
288 (Figure 4). By the week of June 22, toxicity began to rise in far eastern Maine, whereas it was  
289 still relatively low in western Maine. During the week of June 29, toxicity continued to rise in  
290 far eastern Maine, and low-level toxicity was detected nearly coast-wide at the outermost points  
291 and islands. A coast-wide onset of toxicity continued during the week of July 6, reaching its  
292 peak the week of July 13. By the week of July 20 toxicity was on the decline, with highest  
293 values occurring in western Maine where peak toxicities were highest. Toxicity declined further  
294 the week of July 27, and by the week of August 3 the episode was essentially over.

295 Summer 2009 was unusual for *A. fundyense* and shellfish toxicity in the Bay of Fundy,  
296 particularly in Passamaquoddy Bay. Although shellfish in most years become toxic in  
297 Passamaquoddy Bay, it is usually at low levels—although there has been the occasional year that  
298 levels have not gone above the threshold level and shellfish beds have remained opened to  
299 harvesting. Shellfish toxicities prior to 2009 and following 2009 have always been among the  
300 lowest anywhere in the Bay of Fundy. 2009 was the first year since sampling began that *Mya*

301      *arenaria* toxicity values exceeded >1000 µg STX equiv 100 g meat. On June 20 *Mya* toxicity  
302      was 41 µg STX equiv 100 g meat; and the next measurement on July 2 was 4120 µg STX equiv  
303      100 g meat. The following week (July 7) toxicity values had decreased to 441 and on July 14  
304      were 130 µg STX equiv 100 g meat.

305            In a time-series dating back to 1988, *A. fundyense* cells have been observed at Brandy  
306      Cove in Passamaquoddy Bay each year (Figure 5). In all years except 2009, concentrations  
307      were considerably lower than elsewhere in the Bay of Fundy outside Passamaquoddy Bay.  
308      Weekly sampling at Brandy Cove indicated that on June 16, 2009, the concentration of *A.*  
309      *fundyense* was 288 cells l<sup>-1</sup>. By June 23, it had increased to 5616 cells l<sup>-1</sup>, and the following  
310      week on June 30 concentrations had increased to 2.79 x 10<sup>5</sup> cells l<sup>-1</sup>. On July 7, one week later  
311      they had decreased to 2480 cells l<sup>-1</sup>. Interestingly, *A. fundyense* concentrations at Brandy Cove  
312      and shellfish toxicity at Bar Road in Passamaquoddy Bay were the highest for the whole Bay of  
313      Fundy in 2009—a first on record.

314  
315      *3.5 Moored time-series*

316            The McLane PPS time-series of vegetative cells corroborates the highly-ephemeral nature  
317      of the red tide event (Figure 6). *A. fundyense* concentrations began to rise on July 7, peaked at  
318      the very next sample on July 11, and were back to background levels by the 17<sup>th</sup> of July. Note  
319      that the peak concentration observed at 5 m depth is two orders of magnitude smaller than that  
320      measured from near-surface samples obtained on July 10 from *R/V Tioga* (Figure 1). This  
321      suggests the cells were highly concentrated near the surface, above the intake port of the PPS  
322      sampler. This extreme layering of the population was facilitated by calm conditions during that  
323      time, in which wind-driven mixing was minimal. Unfortunately there are no vertical profiles  
324      available within the discolored water to characterize the vertical distribution in detail.

325     3.6 Flow cytometric analysis of the red tide population

326           DNA-associated fluorescence of 1c and 2c *A. fundyense* cells from field samples was  
327       assessed by comparison to a log-phase culture sample that contained abundant 1c (G1 phase) and  
328       scarcer 2c (G2 phase) vegetative cells (Figure 7). The correspondence of fluorescence modes  
329       between the culture and field samples was quite high: all 1c modes from field samples occurred  
330       between 305 and 355 FL2-H units versus 347 in the culture sample, and 2c modes from field  
331       samples occurred between 581 and 695 versus 618 in the culture sample. However, in contrast to  
332       the culture sample, 2c cells were much more abundant than 1c cells in all of the red water  
333       samples taken on July 10 (Figure 1, stations 1-6 near NERACOOS mooring B).

334       The proportion of cells that were 2c was estimated by counting the number of cells in each  
335       sample that had FL2-H measurements greater and less than 450 units. By this criterion, 2c cells  
336       were greater than 95% of those sampled at 4 of the 6 red water stations (1, 2, 5 and 6), and 93%  
337       and 80% of those sampled at the other two (3 and 4, respectively). Station 7, which was outside  
338       the area where discolored water was observed, had a smaller proportion of 2c cells (47%).

339           This indication that a large fraction of the population in the discolored water was  
340       comprised of planozygotes was confirmed with traditional microscopy. The species-specific  
341       counting method described in section 2.3 can be used to distinguish planozygotes from  
342       vegetative cells to the trained eye based on size and staining characteristics. That method of  
343       enumerating planozygotes, albeit less precise, also indicated a high fraction of planozygotes in  
344       the discolored water offshore, and found no evidence of planozygotes at the inshore station (not  
345       shown).

346

347

348    3.7 *Cyst fluxes*

349                 The red-tide event was followed by extremely large fluxes of cysts measured nearby in  
350                 Wilkinson Basin (Figure 8). Peak fluxes of  $75,236 \text{ cysts m}^{-2} \text{ d}^{-1}$  at 95 m and  $292,894 \text{ cysts m}^{-2} \text{ d}^{-1}$   
351                 <sup>1</sup> at 180 m were 4000-5000 times larger than the median fluxes recorded in those time series.  
352                 This cyst flux was the largest measured in all of the traps deployed in the Gulf of Maine in 1995-  
353                 1997 and 2005-2009 as reported in Pilskaln et al. (this issue).

354                 The peak cyst flux at 95 m was a single point corresponding to the sampling interval July  
355                 9-19. A peak occurred simultaneously in the 180 m trap, but the flux persisted at nearly the same  
356                 level for the subsequent sampling interval July 19-30. This is consistent with a longer residence  
357                 time of cysts in the benthic nepheloid layer where near-bottom turbulence resuspends  
358                 sedimentary material (Pilskaln et al., this issue).

359

360    3.8 *Cyst maps*

361                 The abundance of cysts in coastal sediments increased dramatically from 2008 to 2009  
362                 (Figure 9). Integrated abundance in the top 1cm layer of sediment in 2009 was the highest  
363                 observed in the yearly time-series from 2004-2009 (McGillicuddy et al., 2011) and  
364                 measurements thereafter in 2010 and 2011 (Anderson et al., this issue). In addition to the overall  
365                 increase in abundance, the western Gulf of Maine cyst bed (also known as the mid-coast Maine  
366                 cyst bed) spread farther south than in all prior observations. Cyst concentrations in excess of  
367                  $1000 \text{ cysts cm}^{-3}$  extended south and east of Cape Ann, mostly beyond the 200 m isobath. The  
368                 southward tongue of cysts deposited in 2009 had disappeared by the time the same area was  
369                 sampled again in 2010 (Figure 9, right panel), as the southern terminus of the western Gulf of

370 Maine cyst bed returned to its more characteristic position north and east of Cape Ann. See  
371 Anderson et al. (this issue) for more details on cyst dynamics in this region.

372

373 **4. Discussion**

374 What conditions led to the unusual red-tide event observed in July 2009? We examined  
375 the observations described herein, as well as data from the coastal ocean observing system (see  
376 Li et al., this issue), and were unable to discern an unequivocal causal factor. However, one  
377 aspect did stand out as clearly anomalous: wind forcing. As in Li et al. (this issue), we define an  
378 upwelling index  $UI = \frac{\tau_x}{\rho f}$  following the method of Schwing et al. (1996), where  $\tau_x$  is the  
379 alongshore component of the wind stress calculated using Large and Pond (1981),  $\rho$  is the  
380 density, and  $f$  is the local Coriolis parameter. Positive (negative) UI represents upwelling-  
381 (downwelling-) favorable wind conditions, respectively. The cumulative UI (CUI) was computed  
382 by integrating the resulting UI over time (i.e.,  $CUI = \int UI dt$ ) between April 1 and August 1 for  
383 each year, 2004-2011 (Figure 10). The slope of CUI is particularly informative, as upwelling-  
384 (downwelling-) favorable wind conditions are represented by a rising (declining) temporal trend  
385 in CUI. Wind speeds of zero or winds oriented in the cross-shore direction would cause no  
386 change in the CUI, or a slope of zero during such periods. In every year examined except for  
387 2009, the June-July time period is characterized by upwelling-favorable winds driven by the  
388 prevailing summertime southwesterlies in this region. In contrast, winds were generally  
389 downwelling-favorable from late June through early July 2009. A similar downwelling-  
390 favorable trend was evident during the same time period in the eastern Gulf of Maine at  
391 NERACOOS Buoy I (Li et al., this issue), suggesting this was a regional pattern.

392 Wind forcing is a key regulator of *A. fundyense* transport, insofar as upwelling-favorable  
393 winds tend to transport near-coastal populations offshore, and downwelling-favorable winds tend  
394 to transport offshore populations shoreward (Anderson et al., 2005a; Franks and Anderson,  
395 1992a, b; Hetland et al., 2002; McGillicuddy et al., 2003). As such, coincidence of the  
396 anomalous episode of downwelling-favorable winds in late June / early July 2009 with a coast-  
397 wide onset of toxicity (Figure 4) is suggestive of onshore transport of an offshore population  
398 with an alongshore extent spanning the entire Maine coast. Blooms of similar scale have been  
399 observed in the past (Anderson et al., 2005b; Townsend et al., 2001), and their regional scope is  
400 consistent with alongshore advection of coastal populations originating from cyst beds (Figure 9)  
401 in the Bay of Fundy and offshore of mid-coast Maine (Anderson et al., 2005d; McGillicuddy et  
402 al., 2005). Leakiness of the Bay of Fundy gyre has been hypothesized to be a factor influencing  
403 the magnitude of blooms entering the Maine Coastal Current (Aretxabaleta et al., 2008;  
404 Aretxabaleta et al., 2009), but unfortunately there are no measurements to quantify the export of  
405 *A. fundyense* cells from the Bay of Fundy in 2009.

406 Although this event was apparently coast-wide in extent, its visual manifestation appears  
407 to have been confined to the western Gulf of Maine. Direct observations do not permit  
408 delineation of the spatial scale of the discolored water (Figure 1), but satellite data reveal a  
409 pronounced surface expression extending along the coast from western Penobscot Bay to Cape  
410 Ann (Figure 3). This area corresponds directly to the portion of the coastline in which toxicities  
411 were highest (Figure 4).

412 Unfortunately, information about the vertical extent of the population in the discolored  
413 water is scant. That the peak cell concentration observed at the PPS mooring site on July 11 at  
414 5m (Figure 6) was two orders of magnitude smaller than surface samples collected by bucket

415 from R/V *Tioga* on July 10 (Figure 1) suggests that the population was confined to a thin near-  
416 surface layer. However, the non-simultaneity of those measurements constitutes an important  
417 caveat to this inference. Nevertheless, the presence of such high surface concentrations is  
418 indicative of upward swimming, and vertical swimming speeds for *A. fundyense* and similarly-  
419 sized dinoflagellates (diameter ~ 40  $\mu$ ) are typically between 5 and 15 m day<sup>-1</sup> (Anderson and  
420 Stolzenbach, 1985; Bauerfeind et al., 1986; Fauchot et al., 2005; Kamykowski et al., 1992).  
421 Upward swimming in the presence of near-coastal convergence created by downwelling  
422 favorable wind-forcing (Figure 10) would tend to accumulate *A. fundyense* biomass, as has been  
423 demonstrated in a variety of frontal systems (Franks, 1992, 1997).

424 A potential underlying cause of the apparent surface-seeking behavior could have been  
425 the need to aggregate the population to concentrations sufficient to make sexual reproduction  
426 practical (Wyatt and Jenkinson, 1997). Indeed, the predominance of 2c DNA content cells in the  
427 samples from the discolored water (Figure 7) is consistent with a conversion to the sexual phase  
428 of the *A. fundyense* life cycle. However, this is not the only explanation for the high proportion  
429 of 2c cells. Because *A. fundyense* are haplontic (dividing only during its haploid, vegetative  
430 phase), *A. fundyense* may have 2c DNA content either during the G2 phase of mitosis or as  
431 newly-formed planozygotes (Brosnahan et al., this issue). In 5 of the 6 samples from the  
432 discolored water, more than 90% of *A. fundyense* cells were 2c, a ratio that strongly suggests that  
433 at least some of the cells had become planozygotes. The alternative – that the population  
434 consisted only of vegetative cells – is highly improbable because of the preponderance of 2c  
435 cells observed. Furthermore, all of the samples were collected between 1420 and 1702 local  
436 time, when most vegetative *A. fundyense* are in the 1c G1 phase of the cell division cycle rather  
437 than the 2c G2 phase. If it were assumed that all cells were vegetative and undergoing phased

438 division, the minimum growth rate  $\mu$  can be calculated as  $\mu = \frac{1}{t} \ln(1 + f_{max})$ , where  $t$  is time  
439 and  $f_{max}$  is the fraction of the population with 2c DNA content (Chisholm, 1981). The implied  
440 minimum growth rate of  $0.64 \text{ day}^{-1}$  is at the upper limit of this organism's capability (Stock et al.  
441 2005 and references therein), making that an unlikely explanation. Moreover, phased division by  
442 *A. fundyense* more typically occurs at daybreak, not during the late afternoon (Rubin, 1981). For  
443 all these reasons, it is much more likely that a substantial proportion of the 2c cells in these  
444 samples were planozygotes.

445 The unusually large flux of *A. fundyense* cysts observed in Wilkinson Basin (Figure 8)  
446 further attests to the association of the discolored water with a massive sexual reproduction  
447 event. As indicated by the drifter trajectory (Figure 1), the transit time between the area of  
448 discolored water and the sediment trap is approximately ten days. Given sinking rates of *A.*  
449 *fundyense* cysts on the order of  $10 \text{ m day}^{-1}$  (Anderson et al., 1985), arrival at the 95 m sediment  
450 trap along this advective pathway is certainly plausible. Although the cyst flux of 75,236 cysts  
451  $\text{m}^{-2} \text{ d}^{-1}$  observed during July 9-19 at 95 m was the highest of all of the mid-depth deployments  
452 described in Pilskaln et al. (this issue), the total flux measured during this ten-day interval  
453 constitutes less than 10% of what accumulated in the top 1 cm of bottom sediments at this  
454 location between October 2008 and October 2009 (Figure 9). Low-level cyst fluxes throughout  
455 the rest of the year are not nearly able to make up the difference. This implies that the vast  
456 majority of the cysts deposited on the bottom in that location passed through the 95 m depth  
457 horizon elsewhere, perhaps further upstream—and that the cysts passing through 95 m at this  
458 location were deposited further downstream in an area where there was a more modest (ca. 75  
459 cysts  $\text{cm}^{-2}$ ) increase in cyst abundance. The peak flux in the 180 m trap was four times higher  
460 than at 95 m, but it is not possible to partition that increase between lateral inputs and

461 resuspension in the benthic nepheloid layer (see Pilskaln et al. this issue). In any case, the  
462 dramatic accumulation of ca. 1000 cysts  $\text{cm}^{-2}$  east of Cape Ann is consistent with production of  
463 cysts from an overlying population of 100,000 cells  $\text{l}^{-1}$  spread over a 1m-thick layer, assuming  
464 20% success in sexual reproduction (two cells fusing to make one cyst) followed by 100%  
465 deposition in the upper 1 cm of sediment.

466 From an historical perspective, it is interesting to note that the 1972 event was also  
467 associated with cyst formation. Although the cyst stage of *A. fundyense* was not fully described  
468 until later that decade (Anderson and Wall, 1978; Dale, 1977), Mulligan (1973) reported high  
469 concentrations of cysts in water samples taken toward the end of the bloom. Subsequently,  
470 Mulligan (1975) suggested that the abundance of *A. fundyense* cysts in coastal sediments had  
471 increased as a result of the 1972 event, hypothesizing that this reservoir could seed blooms in  
472 future years. Thus, it appears that both the 1972 and 2009 red tides observed in the western Gulf  
473 of Maine involved sexual reproduction and major encystment events.

474

475 **5. Conclusions**

476 The 2009 *A. fundyense* red tide was extraordinary for a number of reasons. To our  
477 knowledge, this is only the second confirmed episode of discolored water in the western Gulf of  
478 Maine directly attributable to *A. fundyense*, the first being associated with the historic bloom of  
479 1972 (Hartwell, 1975; Mulligan, 1973; Sasner et al., 1974). The event was clearly associated  
480 with sexual reproduction, yielding the highest cyst fluxes that have ever been measured in the  
481 region. A large deposit of cysts ensued in coastal sediments, temporarily extending the mid-  
482 coast Maine cyst bed farther south than previously observed.

483           The discolored water appears to have been the southern terminus of a coast-wide  
484 phenomenon, leading to widespread toxicity from the Bay of Fundy to western Maine. The  
485 event was preceded by a period of anomalous downwelling-favorable winds, which favor  
486 outflow from the Bay of Fundy gyre (Aretxabaleta et al., 2008; Aretxabaleta et al., 2009) where a  
487 large source population is typically located. Downwelling-favorable winds also tend to  
488 accelerate the alongshore current, thereby enhancing transport of *A. fundyense* along the coast  
489 into the western Gulf of Maine. A third potential impact of the downwelling-favorable wind  
490 arises from the associated convergence along the coast, which would tend to accumulate upward-  
491 swimming *A. fundyense*.

492           Although the precise mechanisms leading to the red-tide event are not known, one aspect  
493 is clear: it was an extremely-ephemeral phenomenon. A combination of satellite imagery and  
494 rapid-response shipboard surveys constrain the duration of water discoloration to a period of less  
495 than two weeks. Similarly, the 1972 red water event ended abruptly, with *A. fundyense*  
496 disappearing from the plankton within 5-7 days after peak bloom conditions (Sasner et al., 1974).  
497 The short duration of these episodes is particularly humbling from an observational perspective,  
498 insofar as the duration of the event is shorter than the typical interval in between “synoptic”  
499 surveys of bloom dynamics carried out in regional research programs. This begs the question of  
500 how many such events may have been missed in the past due to observing strategies not capable  
501 of resolving them. Fortunately, with the deployment of *in situ* monitoring devices capable of  
502 species-specific measurements (Scholin et al., 2009), future prospects are bright for observing  
503 these highly-transient processes that obviously play an important role in the regional population  
504 dynamics of *A. fundyense* and other harmful algae around the world.

505

506     **Acknowledgments**

507           We are very grateful for the outstanding efforts of the officers, crews, and shore support  
508       of R/V *Oceanus*, R/V *Endeavor*, R/V *Tioga*, and R/V *Gulf Challenger*, as well as the hard work  
509       of all those who participated in the seagoing science teams. Special thanks to the crew of the  
510       R/V *Tioga*, Capt. Ken Houtler, mate Ian Hanley, and relief Capt. Willi Bank for their  
511       extraordinary efforts during the rapid response sampling. Thanks also to Kerry Norton who  
512       assisted with the cell and cyst counts and with preparation of the McLane PPS and to Jon Wood  
513       and Steve Aubrey for their skill during PPS deployment, turnaround during the event, and its  
514       final recovery. Olga Kosnyrev, Valery Kosnyrev, and Keston Smith assisted in data analysis and  
515       figure preparation. We appreciate the efforts of Jason Goldstein and Win Watson at UNH's  
516       Center for Marine Biology, who deployed the drifter in the vicinity of the Isle of Shoals shown in  
517       Figure 1.

518           The R/V *Tioga* sampling effort was facilitated by event response funding from the  
519       National Oceanic Atmospheric Administration (NOAA), National Ocean Service, Center for  
520       Sponsored Coastal Ocean Research, through NOAA Cooperative Agreement NA17RJ1223.  
521       Additional support for follow-up analysis and synthesis was provided by NOAA grant  
522       NA06NOS4780245 for the Gulf of Maine Toxicity (GOMTOX) program and the Woods Hole  
523       Center for Oceans and Human Health through National Science Foundation grants OCE-  
524       0430724 and OCE-0911031 and National Institute of Environmental Health Sciences grant  
525       1P50-ES01274201. This is the Ecology and Oceanography of Harmful Algal Blooms Program  
526       contribution number 738.

527  
528

- 529      **References**
- 530
- 531      Anderson, D.M., Keafer, B.A., Geyer, W.R., Signell, R.P., Loder, T.C., 2005a. Toxic  
532      *Alexandrium* blooms in the western Gulf of Maine: the plume advection hypothesis revisited.  
533      Limnol. Oceanogr. 50, 328-345.
- 534      Anderson, D.M., Keafer, B.A., McGillicuddy, D.J., Martin, J., Norton, K., Pilskahn, C., Smith, J.,  
535      this issue. *Alexandrium fundyense* cysts in the Gulf of Maine: time series of abundance and  
536      distribution, and linkages to past and future blooms. Deep-Sea Research II.
- 537      Anderson, D.M., Keafer, B.A., McGillicuddy, D.J., Mickelson, M.J., Keay, K.E., Libby, P.S.,  
538      Manning, J.P., Mayo, C.A., Whittaker, D.K., Hickey, J.M., He, R., Lynch, D.R., Smith, K.W.,  
539      2005b. Initial observations on the 2005 *Alexandrium fundyense* bloom in southern New England:  
540      general patterns and mechanisms. Deep-Sea Research II, 2856-2876.
- 541      Anderson, D.M., Kulis, D.M., Doucette, G.J., Gallagher, J.C., Balech, E., 1994. Biogeography of  
542      toxic dinoflagellates in the genus *Alexandrium* from the northeastern United States and Canada.  
543      Marine Biology 120, 467-478.
- 544      Anderson, D.M., Kulis, D.M., Keafer, B.A., Gribble, K.E., Marin, R., Scholin, C.A., 2005c.  
545      Identification and enumeration of *Alexandrium* spp. from the Gulf of Maine using molecular  
546      probes. Deep-Sea Research II 52, 2467-2490.
- 547      Anderson, D.M., Lively, J.J., Reardon, E.M., Price, C.A., 1985. Sinking characteristics of  
548      dinoflagellate cysts. Limnology and Oceanography 30, 1000-1009.
- 549      Anderson, D.M., Stock, C.A., Keafer, B.A., Bronzino, A.C., McGillicuddy, D.J., Keller, M.D.,  
550      Thompson, B., Matrai, P.A., Martin, J., 2005d. *Alexandrium fundyense* cyst dynamics in the Gulf  
551      of Maine. Deep-Sea Research II 52, 2522-2542.
- 552      Anderson, D.M., Stolzenbach, K.D., 1985. Selective retention of two dinoflagellates in a well-  
553      mixed estuarine embayment: the importance of vertical migration and surface avoidance. Marine  
554      Ecology Progress Series 25, 39-50.
- 555      Anderson, D.M., Wall, D., 1978. Potential importance of benthic cysts of *Gonyaulax tamarensis*  
556      and *G. excavata* in initiating toxic dinoflagellate blooms. Journal of Phycology 14, 224-234.
- 557      Aretxabaleta, A.L., McGillicuddy, D.J., Smith, K.W., Lynch, D.R., 2008. Model Simulations of  
558      the Bay of Fundy Gyre: 1. Climatological Results. Journal of Geophysical Research 113,  
559      doi:10.1029/2007JC004480.
- 560      Aretxabaleta, A.L., McGillicuddy, D.J., Smith, K.W., Manning, J.P., Lynch, D.R., 2009. Model  
561      Simulations of the Bay of Fundy Gyre: 2. Hindcasts for 2005-2007 Reveal Interannual  
562      Variability in retentiveness. Journal of Geophysical Research 114, doi:10.1029/2008JC004948.
- 563      Association of Official Analytical Chemists, 1984. Association of Official Analytical chemists,  
564      in: Williams, S. (Ed.), Official methods of analysis of the Association of Official Analytical  
565      Chemists. Association of Official Analytical Chemists, Arlington, Virginia, pp. 59-60.

- 566 Bauerfeind, E., Elbrachter, M., Steiner, R., Thronsen, J., 1986. Application of Laser Doppler  
567 Spectroscopy (LDS) in determining swimming velocities in motile phytoplankton. Marine  
568 Biology 93, 323-327.
- 569 Brosnahan, M.L., Farzan, S., Keafer, B.A., Sosik, H.M., Olson, R.J., Anderson, D.M., this issue.  
570 DNA measurements from field populations of the toxic dinoflagellate *Alexandrium tamarense*  
571 Group I using imaging flow cytometry coupled with species-specific rRNA probes. Deep-Sea  
572 Research II.
- 573 Brosnahan, M.L., Kulis, D.M., Solow, A.R., Erdner, D.L., Percy, L., Lewis, J., Anderson, D.M.,  
574 2010. Outbreeding lethality between toxic Group I and nontoxic Group III *Alexandrium*  
575 *tamarense* spp. isolates: Predominance of heterotypic encystment and implications for mating  
576 interactions and biogeography. Deep-Sea Research II 57, 175-189.
- 577 Cetta, C., Anderson, D.M., 1990. Cell cycle studies of the dinoflagellates *Gonyaulax polyedra*  
578 Stein and *Gyrodinium uncatenum* Hulbert during asexual and sexual reproduction. Journal of  
579 Experimental Marine Biology and Ecology 135, 69-83.
- 580 Chisholm, S.W., 1981. Temporal Patterns of Cell Division in Unicellular Algae. Can. Bull. Fish.  
581 Aquat. Sci. 210, 150-181.
- 582 Dale, B., 1977. Cysts of the toxic red-tide dinoflagellate *Gonyaulax excavata* (BRAARUD)  
583 BALECH from Oslofjorden, Norway. Sarsia 63, 29-34.
- 584 Davis, R., 1985. Drifter observations of coastal surface currents during CODE: the method and  
585 descriptive view. Journal of Geophysical Research 90, 4741–4755.
- 586 Doerffer, R., Schiller, H., 2007. The MERIS Case 2 water algorithm. International Journal of  
587 Remote Sensing 28, 517-535.
- 588 Fauchot, J., Levasseur, M., Roy, S., 2005. Daytime and nighttime vertical migrations of  
589 *Alexandrium tamarense* in the St. Lawrence estuary (Canada). Marine Ecology Progress Series  
590 296, 241-250.
- 591 Franks, P.J.S., 1992. Sink or swim: accumulation of biomass at fronts. Marine Ecology -  
592 Progress Series 82, 1-12.
- 593 Franks, P.J.S., 1997. Spatial patterns in dense algal blooms. Limnol. Oceanogr. 42, 1297-1305.
- 594 Franks, P.J.S., Anderson, D.M., 1992a. Alongshore transport of a phytoplankton bloom in a  
595 buoyancy current: *Alexandrium tamarense* in the Gulf of Maine. Marine Biology 112, 153-164.
- 596 Franks, P.J.S., Anderson, D.M., 1992b. Toxic phytoplankton blooms in the southwestern Gulf of  
597 Maine: testing hypotheses of physical control using historical data. Marine Biology 112, 165-  
598 174.
- 599 Hansen, D.D., Poulain, P.-M., 1996. Quality control and interpolations of WOCE-TOGA drifter  
600 data. Journal of Atmospheric and Oceanic Technology 13, 900-909.

- 601 Hartwell, A.D., 1975. Hydrographic factors affecting the distribution and movement of toxic  
602 dinoflagellates in the western Gulf of Maine, in: LoCicero, V.R. (Ed.). Proceedings of the First  
603 International Conference on Toxic Dinoflagellate Blooms. Massachusetts Science and  
604 Technology Foundation (MIT Sea Grant Program Report No. MITSG 75-8), pp. 47-68.
- 605 Hetland, R.D., McGillicuddy, D.J., Signell, R.P., 2002. Cross-frontal entrainment of plankton  
606 into a buoyant plume: the frog tongue mechanism. Journal of Marine Research 60, 763-777.
- 607 Honjo, S., Doherty, K.W., 1988. Large aperture time-series sediment traps; design objectives,  
608 construction and application. Deep-Sea Research I 35, 133-149.
- 609 Kamykowski, D., Reed, R.E., Kirkpatrick, G.J., 1992. Comparison of sinking velocity,  
610 swimming velocity, rotation and path characteristics among six marine dinoflagellate species.  
611 Marine Biology 113, 319–328.
- 612 Large, W.G., Pond, S., 1981. Open ocean momentum flux measurements in moderate to strong  
613 winds. Journal of Physical Oceanography 11, 329-336.
- 614 Li, Y., He, R., McGillicuddy, D.J., this issue. Seasonal and Interannual Variability in Gulf of  
615 Maine Hydrodynamics: 2002-2011. Deep-Sea Research II.
- 616 Manning, J.P., McGillicuddy Jr, D.J., Pettigrew, N.R., Churchill, J.H., Incze, L.S., 2009. Drifter  
617 observations of the Gulf of Maine Coastal Current. Continental Shelf Research 29, 835-845.
- 618 Martin, J.L., LeGresley, M.M., Hanke, A., Page, F.H., 2008. *Alexandrium fundyense* - Red  
619 Tides, PSP Shellfish Toxicity, Salmon Mortalities and Human Illnesses in 2003-04 – Before and  
620 After, in: Moestrup, O. (Ed.). Proceedings of the 12th International Conference on Harmful  
621 Algae. International Society for the Study of Harmful Algae and Intergovernmental  
622 Oceanographic Commission of UNESCO, Copenhagen, pp. 206-208.
- 623 Martin, J.L., White, A.A., 1988. Distribution and abundance of the toxic dinoflagellate  
624 *Gonyaulax excavata* in the Bay of Fundy. Can. J. Fish. Aquat. Sci. 45, 1968-1975.
- 625 McGillicuddy, D.J., Anderson, D.M., Lynch, D.R., Townsend, D.W., 2005. Mechanisms  
626 regulating the large-scale seasonal fluctuations in *Alexandrium fundyense* populations in the Gulf  
627 of Maine: results from a physical-biological model. Deep-sea Research II 52, 2698-2714.
- 628 McGillicuddy, D.J., Signell, R.P., Stock, C.A., Keafer, B.A., Keller, M.D., Hetland, R.D.,  
629 Anderson, D.M., 2003. A mechanism for offshore initiation of harmful algal blooms in the  
630 coastal Gulf of Maine. Journal of Plankton Research 25, 1131-1138.
- 631 McGillicuddy, D.J., Townsend, D.W., He, R., Keafer, B.A., Kleindinst, J.L., Li, Y., Manning,  
632 J.P., Mountain, D.G., Thomas, M.A., Anderson, D.M., 2011. Suppression of the 2010  
633 *Alexandrium fundyense* bloom by changes in physical, biological, and chemical properties of the  
634 Gulf of Maine. Limnology and Oceanography 56, 2411–2426.
- 635 Mulligan, H.F., 1973. Probable Causes for the 1972 Red Tide in the Cape Ann Region of the  
636 Gulf of Maine. Journal of the Fisheries Research Board of Canada 30, 1363-1366.

- 637 Mulligan, H.F., 1975. Oceanographic factors associated with New England red tide blooms, in:  
638 LoCicero, V.R. (Ed.). Proceedings of the First International Conference on Toxic Dinoflagellate  
639 Blooms. Massachusetts Science and  
640 Technology Foundation (MIT Sea Grant Program Report No. MITSG 75-8), pp. 23-40.
- 641 Pfiester, L.A., Anderson, D.M., 1987. Dinoflagellate Reproduction, in: Taylor, F.J.R. (Ed.), The  
642 Biology of the Dinoflagellates. Wiley-Blackwell, pp. 610–648.
- 643 Pilskaln, C.H., Anderson, D.M., McGillicuddy, D.J., Keafer, B.A., Hayashi, K., Norton, K., this  
644 issue. Spatial and temporal variability of *Alexandrium* cyst fluxes in the Gulf of Maine:  
645 Relationship to seasonal particle export and resuspension. Deep-Sea Research II.
- 646 Rubin, C., 1981. Measurements of in situ growth rates of *Gonyaulax tamarensis*: the New  
647 England red tide organism. M.S. Thesis, Massachusetts Institute of Technology, Cambridge,  
648 MA, pp. 1-54.
- 649 Sasner, J., Ikawa, M., Barrett, B.E., 1974. ‘Red tide’ in the Southern Gulf of Maine, USA.  
650 Biological Conservation 6, 76-78.
- 651 Scholin, C., Doucette, G., Jensen, S., Roman, B., Pargett, D., Marin, R., Preston, C., Jones, W., J.  
652 Feldman, Everlove, C., Harris, A., Avarado, N., Massion, E., Birch, J., Greenfield, D., Wheeler,  
653 K., Vrijenhoek, R., Mikulski, C., Jones, K., 2009. Remote detection of marine microbes, small  
654 invertebrates, harmful algae and biotoxins using the Environmental Sample Processor (ESP).  
655 Oceanography 22, 158-167.
- 656 Scholin, C.A., Hallegraeff, G.M., Anderson, D.M., 1995. Molecular evolution of the  
657 *Alexandrium tamarense* 'species complex' (Dinophyceae): Dispersal in the North American and  
658 West Pacific regions. Phycologia 34, 472-485.
- 659 Schwing, F.B., O’Farrell, M., Steger, J.M., Baltz, K., 1996. Coastal upwelling indices, West  
660 Coast of North America, 1946 – 1995, NOAA Technical Memo. NOAA-TM-NMFS-SWFSC-  
661 231, p. 144.
- 662 Stock, C.A., McGillicuddy, D.J., Solow, A.R., Anderson, D.M., 2005. Evaluating hypotheses for  
663 the initiation and development of *Alexandrium fundyense* blooms in the western Gulf of Maine  
664 using a coupled physical-biological model. Deep-Sea Research II 52, 2715-2744.
- 665 Taroncher-Oldenburg, G., Kulis, D., Anderson, D.M., 1997. Toxin variability during the cell  
666 cycle of the dinoflagellate *Alexandrium fundyense*. Limnology and Oceanography, 1178–1188.
- 667 Townsend, D.W., Pettigrew, N.R., Thomas, A.C., 2001. Offshore blooms of the red tide  
668 dinoflagellate *Alexandrium* sp., in the Gulf of Maine. Continental Shelf Research 21, 347-369.
- 669 Wyatt, T., Jenkinson, I.R., 1997. Notes on *Alexandrium* population dynamics. Journal of  
670 Plankton Research 19, 551-575.
- 671
- 672

673 **Figure Captions**

674  
675 Figure 1. Dots north of 43°N: surface *A. fundyense* concentrations (cells l<sup>-1</sup>) observed on July 10,  
676 2009 (whole cell counts). Station numbers (in parentheses) precede the cell counts, and the  
677 percentage of planozygotes follows in brackets. Map, dots, and plus signs south of 43°N: surface  
678 *A. fundyense* concentrations observed on R/V *Tioga* 383 July 12, 2009 (live counts). Black crosses  
679 indicate the locations of NERACOOS mooring “B” where the McLane PPS sampler was located,  
680 and the Wilkinson Basin “WB” sediment trap. Trajectory of surface drifter #97201 released on  
681 July 9 is plotted as a gray line, with dates provided every two days along track.

682  
683 Figure 2. Surface *A. fundyense* concentrations observed on R/V *Tioga* 386 July 19-23, 2009  
684 (live counts). Inset shows a zoom view of the near shore underway data collected at the northern  
685 terminus of the survey.

686  
687 Figure 3. Top: MERIS “Algal 2” image for July 9, 2009 depicting chlorophyll for case-2 waters.  
688 White crosses indicate the positions of *A. fundyense* measurements in the discolored water  
689 (Figure 1). Bottom: time-series of images zoomed into the area of discolored water.

690  
691 Figure 4. Weekly toxicity maps for the coast of Maine from mid-June to early August, 2009.

692  
693 Figure 5. *A. fundyense* concentrations from weekly sampling at Brandy Cove, Passamaquoddy  
694 Bay from 1988-2011.

695  
696 Figure 6. Time-series of *A. fundyense* cell concentrations at 5 m depth collected from the  
697 McLane PPS moored at 43° 11'N, 70° 26'W (Figure 1, “B”).

698  
699 Figure 7. Relative frequency of FL2-H (DNA-associated) fluorescence from flow cytometry  
700 analysis of a log-phase culture of vegetative *A. fundyense* (top curve) and red tide samples taken  
701 from stations 1-7 on July 10 (Figure 1). The frequency distributions have been smoothed and are  
702 plotted as deviations from zero (e.g. no cells were observed with FL2-H fluorescence less than  
703 200). Stations 1-6 are the offshore locations where *A. fundyense* concentrations were sufficient to  
704 discolor the water (highest *A. fundyense* concentration at Station 1), whereas station 7 was the  
705 near-coastal location where the concentration of *A. fundyense* was 25,690 cells l<sup>-1</sup>.

706  
707 Figure 8. Cysts fluxes measured at the northern Wilkinson Basin site (Figure 1, “WB”) at 95 m  
708 (top) and 180 m (bottom). Open circles indicate zero cyst flux/no cysts collected in the trap cup  
709 during the particular collection period. Peak cyst fluxes in 2009 occurred in consecutive samples  
710 4-7 of the deployment starting in June 2009. The time intervals for samples 4-7 were: July 9-19,  
711 July 19-30, July 30 - August 9, August 9-19. Note that each dot in the time-series is plotted at the  
712 beginning of each sampling interval. Modified from Pilskaln et al. (this issue).

713  
714 Figure 9. *A. fundyense* cyst abundance in the upper 1cm layer of sediment observed in October  
715 2008 (left), 2009 (middle), and 2010 (right). Black dots denote the locations of sediment  
716 samples used to construct the maps. Location of the Wilkinson Basin “WB” sediment trap is  
717 indicated by a black cross.

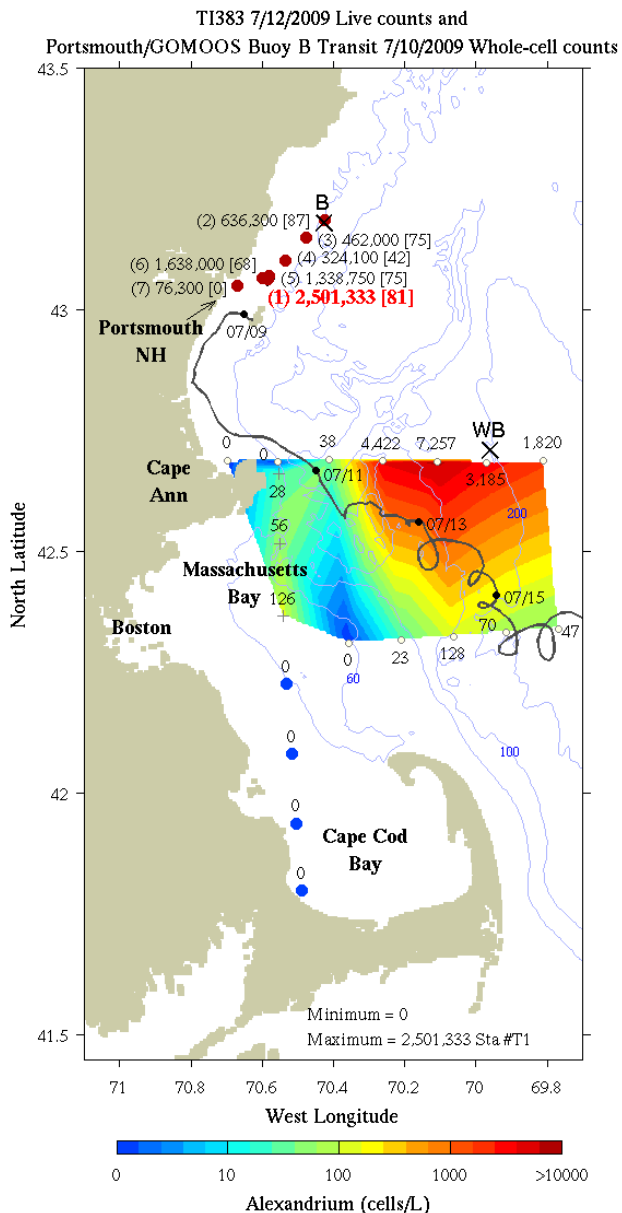
719 Figure 10. Time-series of cumulative upwelling index ( $\text{m}^3 (\text{100m coastline})^{-1} \text{ d}^{-1}$ ) for 2004-2011 at  
720 NERACOOS buoy B (see Figure 1 for buoy location). Vertical arrows bracket the time period of  
721 unusual downwelling during the summer of 2009.

722

723

724  
725  
726  
727

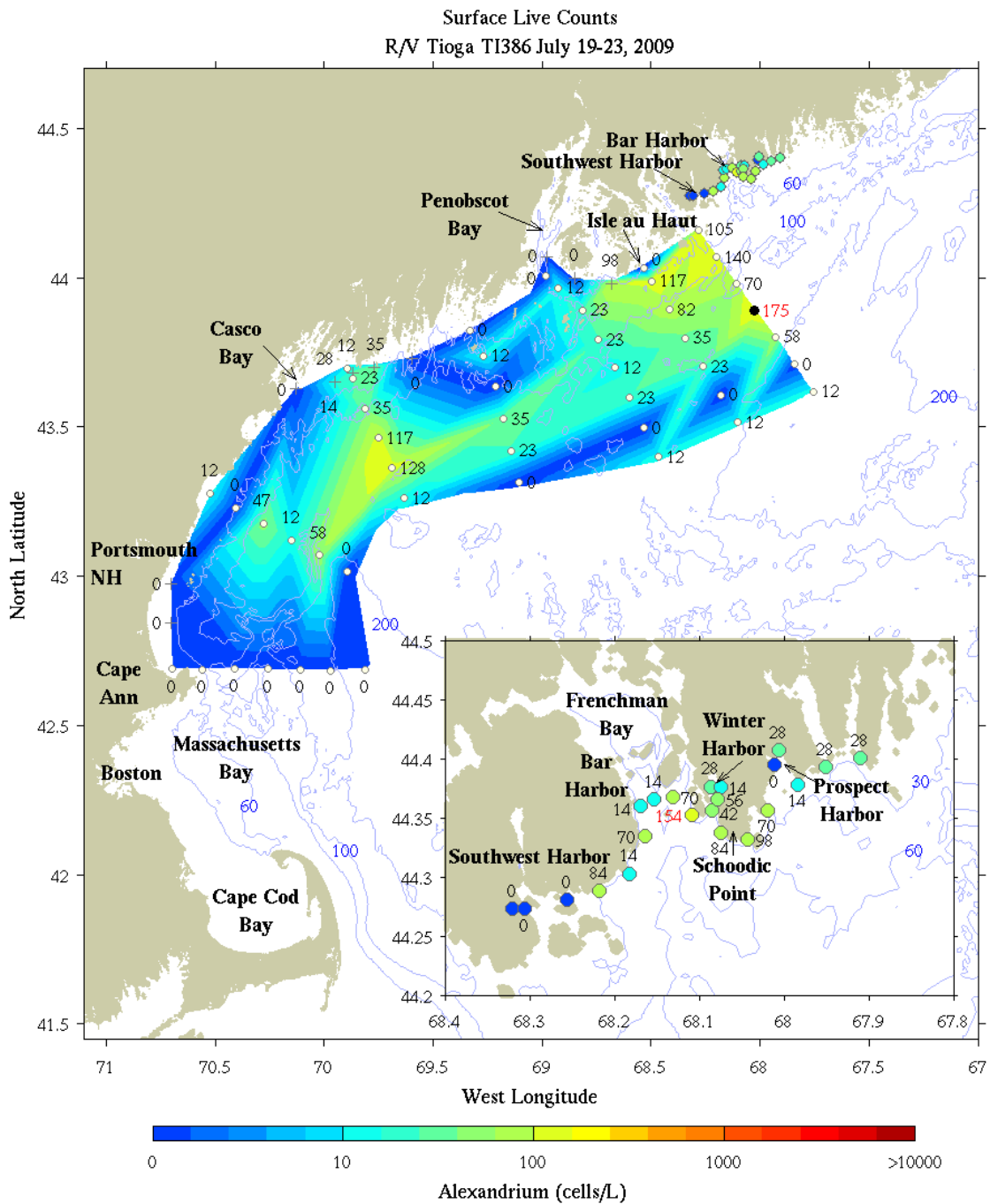
McGillicuddy et al., Figure 1.



728  
729 Figure 1. Dots north of 43°N: surface *A. fundyense* concentrations (cells  $\text{L}^{-1}$ ) observed on July  
730 10, 2009 (whole cell counts). Station numbers (in parentheses) precede the cell counts, and the  
731 percentage of planozygotes follows in brackets. Map, dots, and plus signs south of 43°N:  
732 surface *A. fundyense* concentrations observed on R/V *Tioga* 383 July 12, 2009 (live counts).  
733 Black crosses indicate the locations of NERACOOS mooring "B" where the McLane PPS  
734 sampler was located, and the Wilkinson Basin "WB" sediment trap. Trajectory of surface drifter  
735 #97201 released on July 9 is plotted as a gray line, with dates provided every two days along  
736 track.

737  
738

McGillicuddy et al., Figure 2.

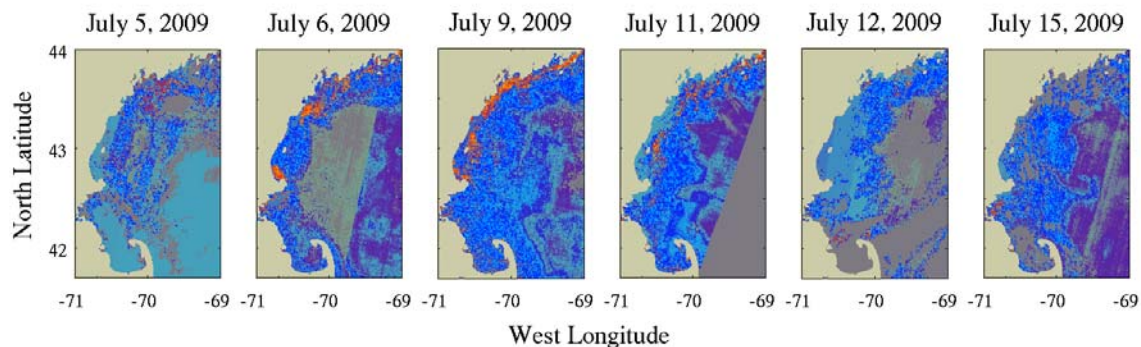
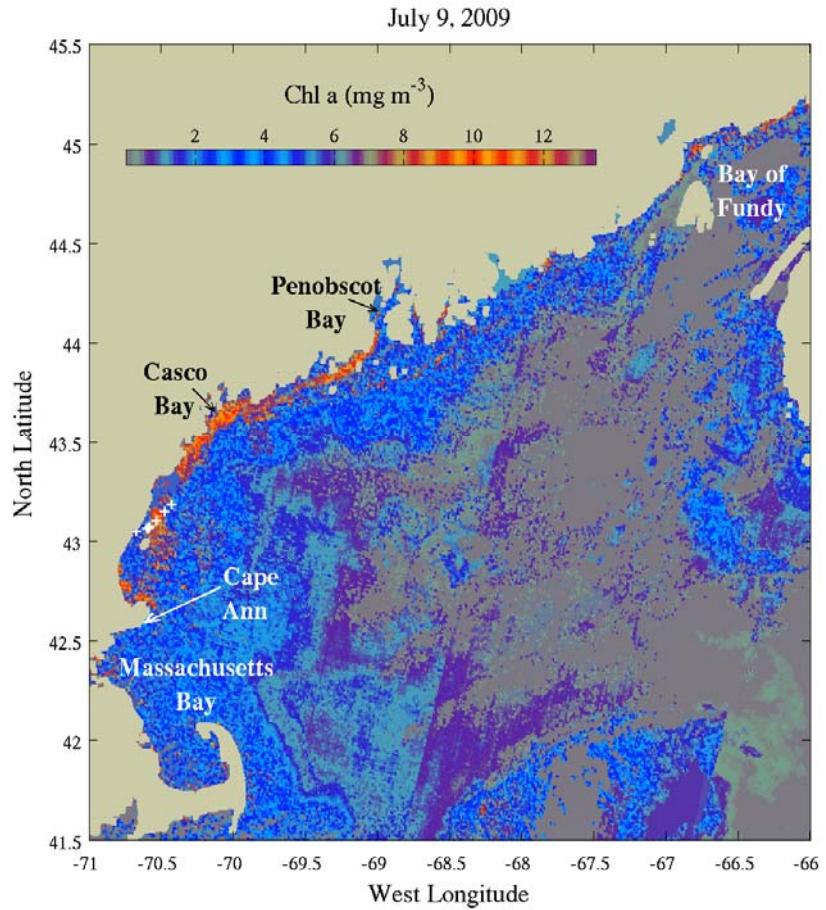


739  
740  
741  
742  
743  
744  
745

Figure 2. Surface *A. fundyense* concentrations observed on R/V *Tioga* 386 July 19-23, 2009 (live counts). Inset shows a zoom view of the near shore underway data collected at the northern terminus of the survey.

746  
747

McGillicuddy et al., Figure 3.



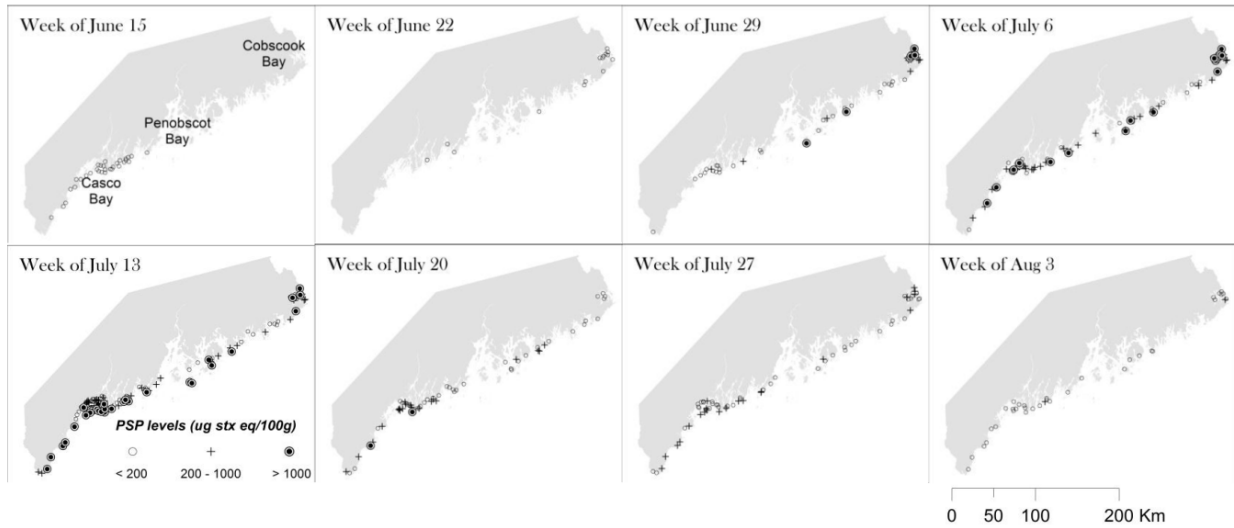
748  
749  
750

751 Figure 3. Top: MERIS "Algal 2" image for July 9, 2009 depicting chlorophyll for case-2 waters.  
752 White crosses indicate the positions of *A. fundyense* measurements in the discolored water  
753 (Figure 1). Bottom: time-series of images zoomed into the area of discolored water.

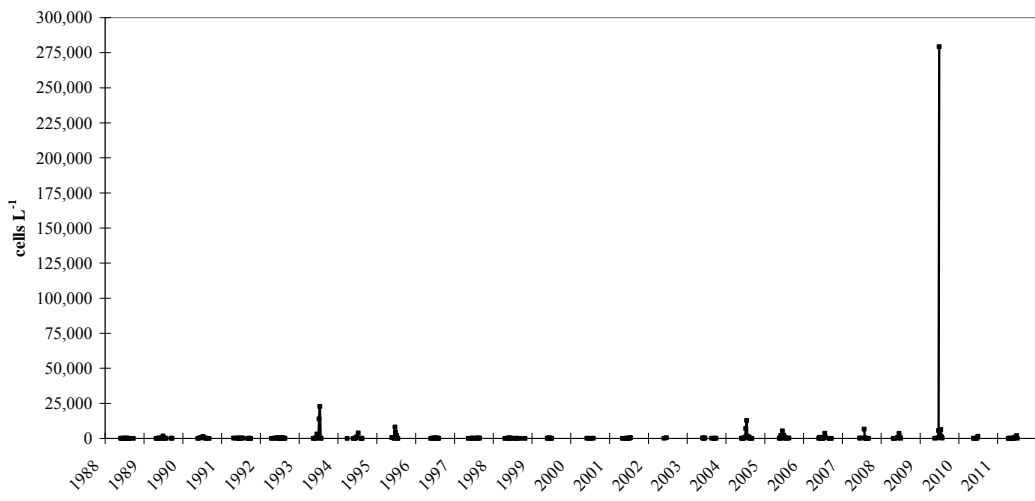
754  
755

756  
757  
758

McGillicuddy et al., Figure 4.



759  
760  
761 Figure 4. Weekly toxicity maps for the coast of Maine from mid-June to early August, 2009.  
762



764

765

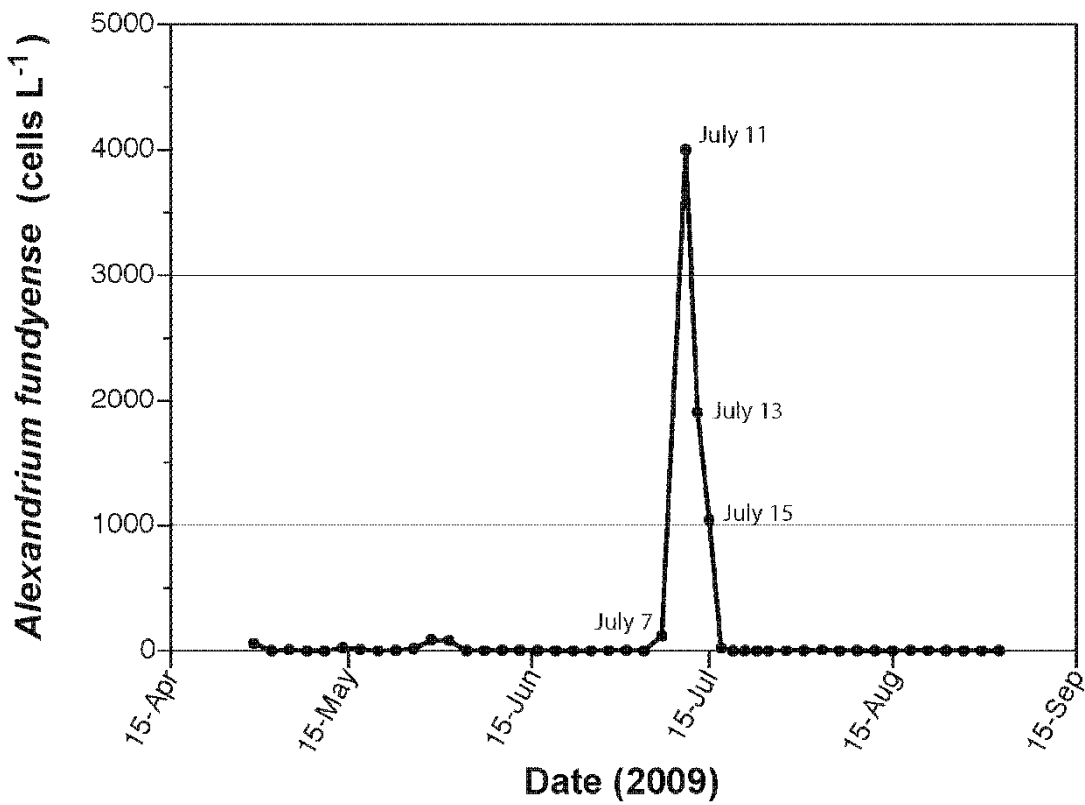
766 Figure 5. *A. fundyense* concentrations from weekly sampling at Brandy Cove, Passamaquoddy  
767 Bay from 1988-2011.

768

769

770  
771

McGillicuddy et al., Figure 6.

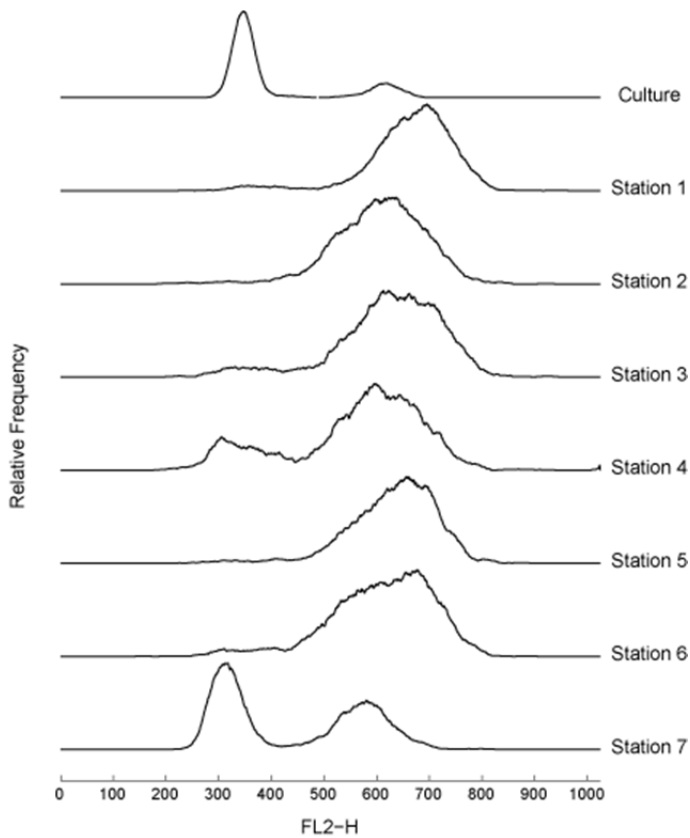


772  
773  
774  
775  
776  
777

Figure 6. Time-series of *A. fundyense* cell concentrations at 5 m depth collected from the McLane PPS moored at 43° 11'N, 70° 26'W (Figure 1, "B").

778  
779  
780  
781

McGillicuddy et al., Figure 7.

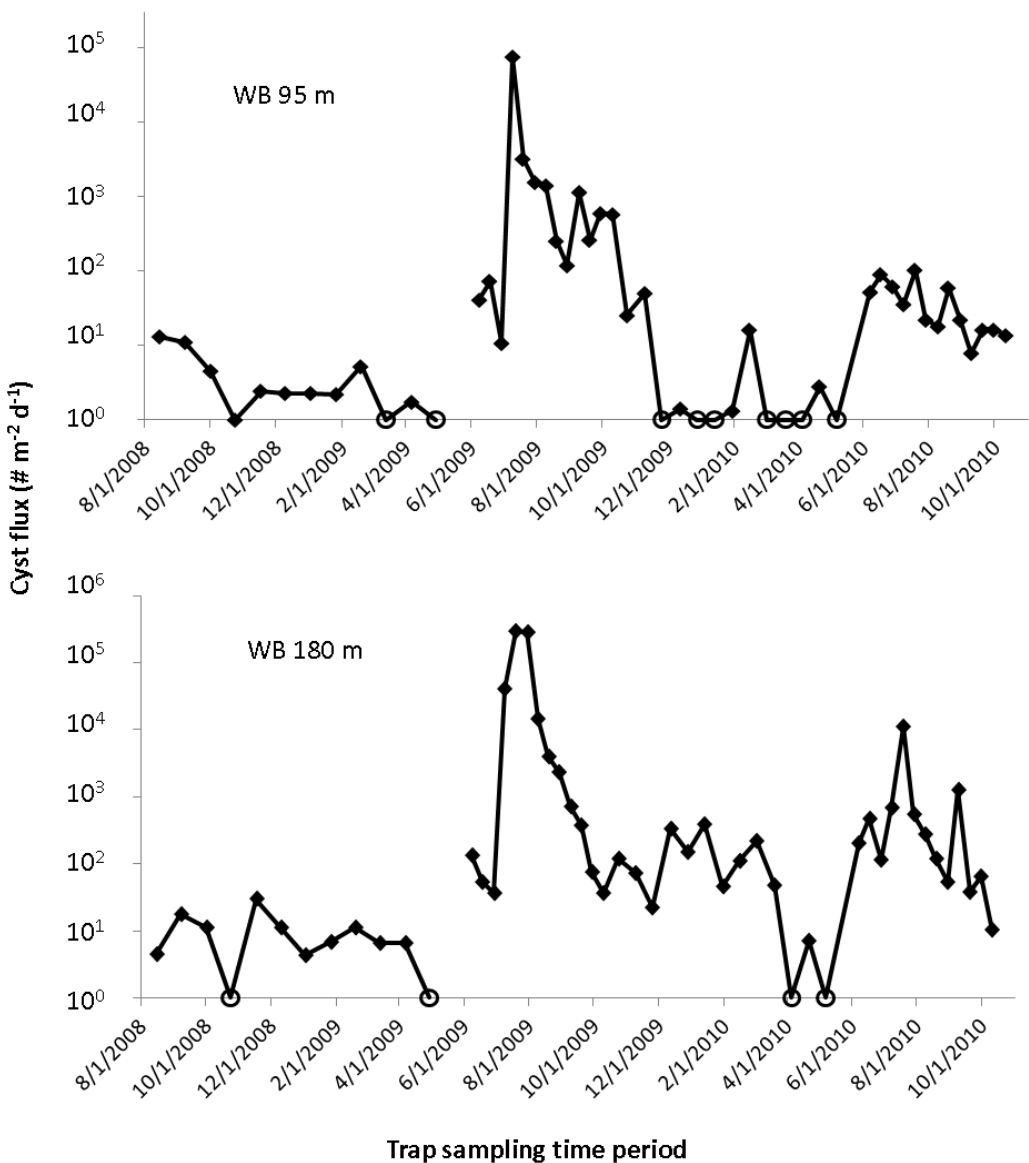


782  
783  
784  
785  
786  
787  
788  
789  
790  
791  
792

Figure 7. Relative frequency of FL2-H (DNA-associated) fluorescence from flow cytometry analysis of a log-phase culture of vegetative *A. fundyense* (top curve) and red tide samples taken from stations 1-7 on July 10 (Figure 1). The frequency distributions have been smoothed and are plotted as deviations from zero (e.g. no cells were observed with FL2-H fluorescence less than 200). Stations 1-6 are the offshore locations where *A. fundyense* concentrations were sufficient to discolor the water (highest *A. fundyense* concentration at Station 1), whereas station 7 was the near-coastal location where the concentration of *A. fundyense* was  $25,690 \text{ cells l}^{-1}$ .

793  
794  
795

McGillicuddy et al., Figure 8.

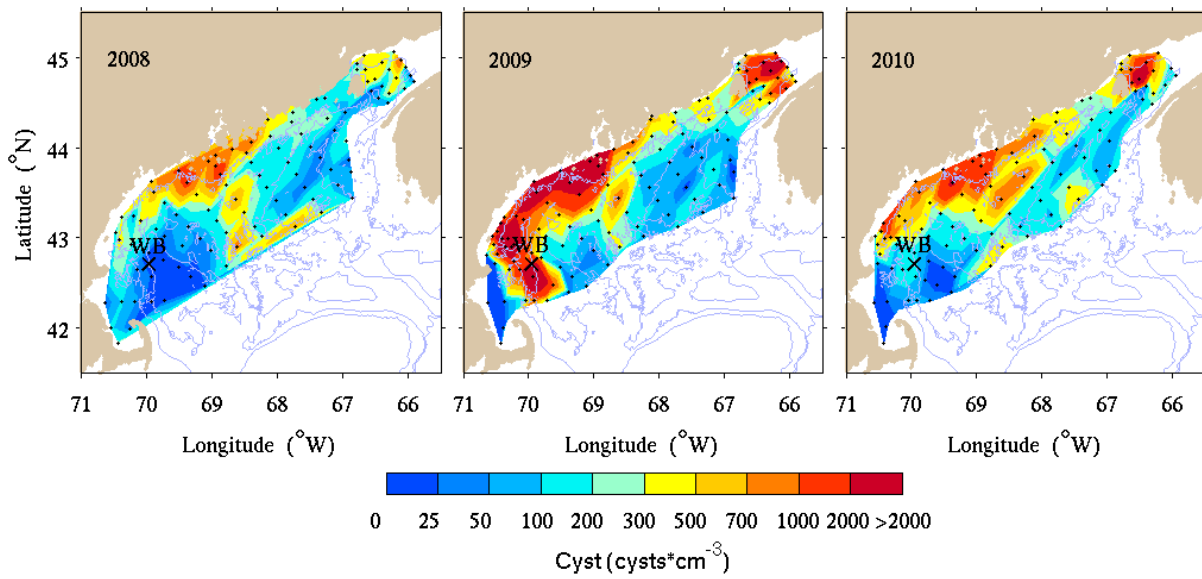


796  
797  
798

799 Figure 8. Cysts fluxes measured at the northern Wilkinson Basin site (Figure 1, “WB”) at 95 m  
800 (top) and 180 m (bottom). Open circles indicate zero cyst flux/no cysts collected in the trap cup  
801 during the particular collection period. Peak cyst fluxes in 2009 occurred in consecutive samples  
802 4-7 of the deployment starting in June 2009. The time intervals for samples 4-7 were: July 9-19,  
803 July 19-30, July 30 - August 9, August 9-19. Note that each dot in the time-series is plotted at  
804 the beginning of each sampling interval. Modified from Pilskaln et al. (this issue).

805  
806  
807

McGillicuddy et al., Figure 9.

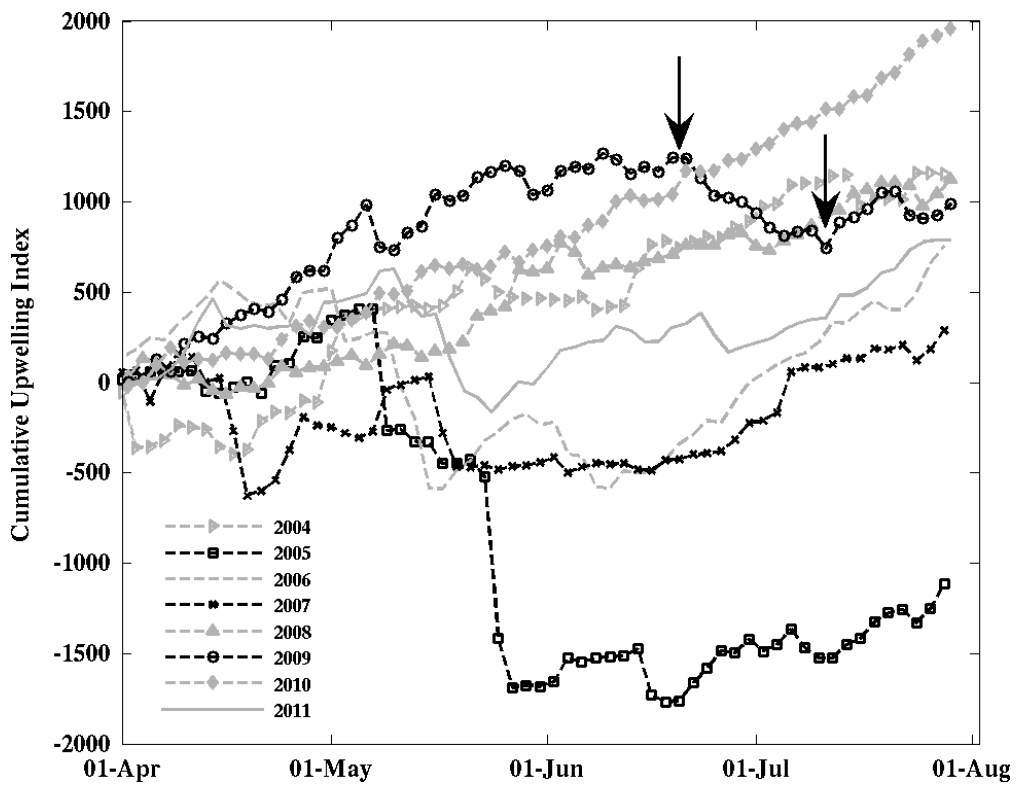


808  
809  
810  
811  
812  
813  
814  
815  
816  
817  
818

Figure 9. *A. fundyense* cyst abundance in the upper 1 cm layer of sediment observed in October 2008 (left), 2009 (middle), and 2010 (right). Black dots denote the locations of sediment samples used to construct the maps. Location of the Wilkinson Basin “WB” sediment trap is indicated by a black cross.

819  
820

McGillicuddy et al., Figure 10.



821  
822

823

824 Figure 10. Time-series of cumulative upwelling index ( $m^3 (100m \text{ coastline})^{-1} d^{-1}$ ) for 2004-2011 at  
825 NERACOOS buoy B (see Figure 1 for buoy location). Vertical arrows bracket the time period of  
826 unusual downwelling during the summer of 2009.  
827  
828  
829